Proceedings of the 11th ICPMG 2026
11th International Conference on Physical Modelling in Geotechnics
8-12 June 2026, Zurich, Switzerland

Shaking table tests using geotechnical centrifuge to investigate non-linear behavior of sandy ground during Nankai Trough simulated earthquake

H. Iwai
Taisei Corporation, 344-1, Nase-cho, Totsuka-ku, Yokohama 245-0051, Japan, iwihzm00@pub.taisei.co.jp

Y. Ikami, K. Shibata, H. Uno, H. Funahara, T. Fujiwara, S. Ishizaki
Taisei Corporation, 344-1, Nase-cho, Totsuka-ku, Yokohama 245-0051, Japan, ikmysh00@pub.taisei.co.jp, sbtkit00@pub.taisei.co.jp, hiroki-u@ce.taisei.co.jp, hideki.funahara@sakura.taisei.co.jp, tadafumi.fujiwara@sakura.taisei.co.jp, sada.ishizaki@sakura.taisei.co.jp

ABSTRACT: In Japan, a Nankai Trough megathrust earthquake is predicted to occur in the near future. If such an earthquake, with large acceleration amplitudes and a high proportion of long-period components, were to occur, non-linear behavior of ground such as strain-dependent stiffness reduction and liquefaction, which significantly affect the seismic responses of buildings and underground structures, would occur. In 2024, a new geotechnical centrifuge was introduced at our research facility, and the shaking table equipped with the centrifuge can reproduce large-amplitude and long-period seismic motion. Therefore, we conducted shaking table tests on dry and saturated sandy soil with medium and high density to investigate the non-linear behavior of sandy soil during the large earthquake. In the case of dry sand, the results of the tests indicate that shear strain and stiffness-reduction rate during an earthquake increases as relative density decreases. In the case of saturated sand, the possibility of liquefaction occurrence at depths deeper than G.L.-20m is verified and the generation of pulsed acceleration due to cyclic mobility is notably evident in the high-density case. Furthermore, we conducted reproduction simulations using FEM for both cases. The results of the simulations generally agree with the results of the tests. In particular, for the simulations targeting saturated sand, incorporating groundwater movement enables reproduction of the development and dissipation processes of excess pore water pressure during long-duration earthquakes such as the input wave in these tests.

1 INTRODUCTION

In Japan, where earthquake disasters occur frequently, seismic design of buildings is essential. To perform detailed seismic design, understanding the non-linear behavior of ground during a large earthquake, which is significantly related to the occurrence of ground displacement that greatly affects the response of pile foundations and the magnitude of input acceleration to a superstructure, is critically important.

While it is possible to verify the non-linear behavior of ground during earthquakes with large-amplitude accelerations and a high proportion of long-period components, such as a Nankai Trough earthquake likely to occur in Japan in the near future (The Headquarters for Earthquake Research Promotion (2025)), through numerical simulations, it has not been possible for us to verify the behavior experimentally. It is because that performance of the shaking table equipped with the geotechnical centrifuge which was previously available at our research facility (Nagura et al. (1992)) was not sufficient to reproduce the wave mentioned above. In 2024, a new geotechnical centrifuge was introduced and the shaking table equipped with the new centrifuge can reproduce large-amplitude and long-period seismic motion. Therefore, we conducted shaking table tests on dry and saturated sandy soil with medium and high density to investigate the non-linear behavior of sandy soil during the large earthquake.

First, the outline of the new centrifuge is explained, and the reproduction results of the target seismic wave are shown. Second, the outlines of a series of the centrifugal shaking tests and of the reproduction simulations on the tests are explained. Finally, the results of the tests are analysed from the perspective of how differences in relative density affect the seismic behavior of ground, and the validity of the simulation method is examined by comparing these results with the results of the simulations.

Figure 1. Appearance of the new geotechnical centrifuge.

Table 1. Basic performance of the new geotechnical centrifuge.

Effective rotation radius (m)	4.0
Maximum centrifugal acceleration (G)	Dynamic : 75 Static : 100
Maximum size of the model (m)	Dynamic : L1.0×W1.0×H1.0 Static : L2.0×W2.0×H2.0

Table 2. Performance of the shakers.

Maximum acceleration (G)	Horizontal	For large-amplitude sesmic motion	60
		For long-period sesmic motion	20
	Vertical		60
Maximum velocity (cm/s)	Horizontal	For large-amplitude sesmic motion	125
		For long-period sesmic motion	200
	Vertical		50
Maximum amplitude (mm)	Horizontal	For large-amplitude sesmic motion	10
		For long-period sesmic motion	20
	Vertical		5

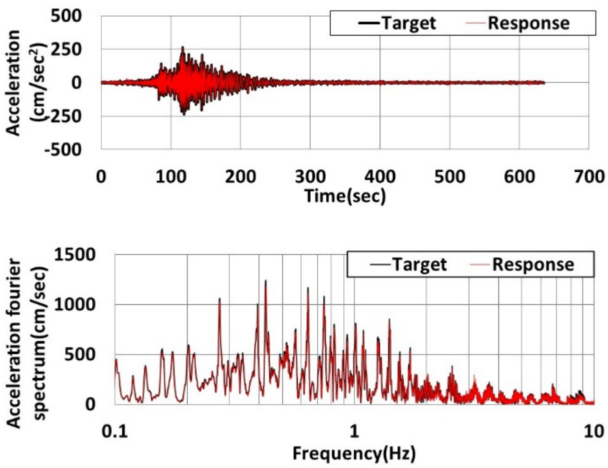

Figure 2. Comparison of the target and response.

2 NEW GEOTECHNICAL CENTRIFUGE

Figure 1 shows the appearance of the new geotechnical centrifuge. The effective rotation radius is longer, and the maximum size of the model is larger than that of the old centrifuge at our facility (Nagura et al. (1992)). Table 1 shows the basic performance of the new geotechnical centrifuge.

Table 2 shows the performance of the shakers. There are two types of shakers in the horizontal direction (one for large-amplitude seismic motion and the other for long-period seismic motion), which are selected depending on the application. The shaker for large-amplitude seismic motion can reproduce seismic motions with amplitudes 1.5 times those of motions predicted to occur extremely rarely in Japan (on the order of once in several hundred years). This feature also applies to the shaker in the vertical direction. Moreover, the shaker for long-period seismic motion can reproduce waves containing longer-period components and exhibiting larger displacement amplitudes than the other horizontal shaker.

Figure 2 shows a comparison of the time history and the Fourier spectrum between the target input seismic wave used in the shaking table tests and the shaking table response after correcting the transfer function to reproduce the target wave with a counterweight placed on the shaking table. These are in good agreement and demonstrate the high reproducibility of the shaking table.

3 OUTLINE OF SHAKING TABLE TESTS

Table 3 shows the test cases and Figure 3 shows the test models. In these tests, Toyoura sand was used as the material for ground models. Table 4 shows the properties of Toyoura sand. In CASE1, it was used as a dry sandy soil model, and in CASE2, it was used as a saturated sandy soil model. This case classification aims to verify how ground responses differ depending on whether the occurrence of liquefaction is considered. In CASE2, silicone oil with a viscosity 50 times that of water was used as the pore fluid to satisfy the similarity rules. The centrifugal acceleration is 50g. The figures and tables below show values at real scale. Furthermore, for each case, two patterns of relative density (medium density and high density) were specified to investigate the effect of relative density on the non-linear behavior of ground.

These models were shaken using the wave shown in Figure 2. Additionally, to comprehend the natural period of ground, the models were shaken using micro white noise before and after the main shaking.

Table 3. Test cases.

CASE	Dry or Satureted	Relative density (%)
1-1	Dry	69
1-2		91
2-1	Saturated	60
2-2		91

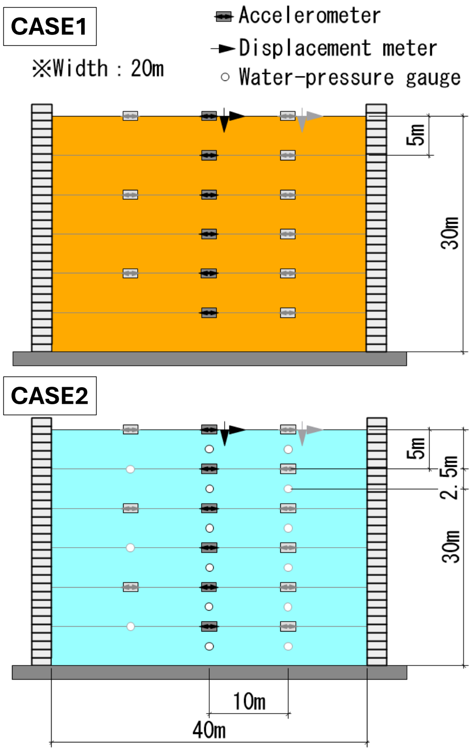

Figure 3. Test models.

Table 4. Properties of Toyoura sand.

Average grain shape (mm)	0.1756
Uniformity coefficient	1.460
Soil particle density (g/cm^3)	2.657
Dry density (g/cm^3)	Max:1.644 Min:1.378

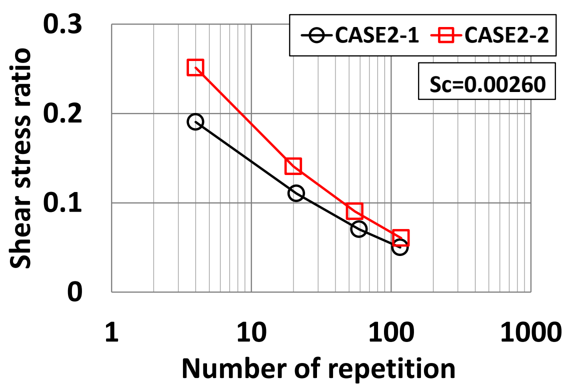

Figure 4. Liquefaction strength curves.

4 OUTLINE OF SIMULATION

To reproduce the results of the tests, simulations using FEM were conducted. The simulation model is a one-dimensional soil column model that discretizes a 30m-thick layer into 1m segments using plain-strain elements. The simulation program is TDAPIII. A two-phase governing equation is implemented in the program, which enables the evaluation of groundwater movement between elements. In the simulation on CASE2, u-w formulation (Ghaboussi et al. (1984)) is adopted as the governing equation.

The following describes the boundary conditions of the simulation model. In CASE1, horizontal and vertical displacements of the soil skeleton at the same depth are tied, and displacements of that at the bottom of the model are fixed. In CASE2, as for the pore water, horizontal displacements at the same depth are tied in addition to the condition applied to the soil skeleton in CASE1.

In CASE1, the initial shear stiffness of ground was determined so that the natural period of the simulation model generally matches the natural period calculated from the results of the tests, as described later. Furthermore, the initial shear stiffness is proportional to the square root of the effective confining pressure corresponding to depth. The hyperbolic model (Hardin et al. (1972)) is used to evaluate the non-linear behavior of the ground, and the reference strain is set for each element according to the confining pressure, referring to the dynamic deformation characteristics of Toyoura sand (Kokusho. (1980)).

In CASE2, Stress-Density model (Cubrinovski et al. (1998)) is adopted as the constitutive law for the soil skeleton which expresses the stress-strain relationship of liquefiable sandy soil. The parameters of Stress-Density model are the same as those in the literature (Cubrinovski et al. (1998)), except for the dilatancy parameter S_c which is used to control the plastic strain dependency of the stress-dilatancy relationship. S_c is calibrated so that the results of the tests can be reproduced in the simulations. Figure 4 shows the liquefaction strength curves. In this simulation, a 650-second dynamic analysis is conducted, followed by a 1500-second consolidation analysis.

5 RESULTS OF TESTS AND SIMULATIONS

5.1 Behavior of dry sand

5.1.1 Natural period of ground

To verify changes in ground properties due to the main shaking and to compare with the natural period of

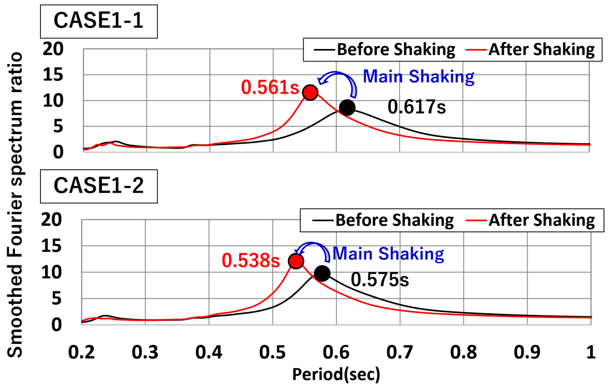

Figure 5. Fourier spectrum ratio (dry sand).

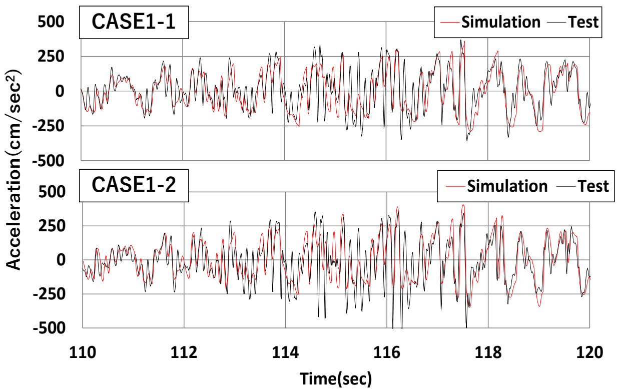

Figure 6. Acceleration of the ground surface (dry sand).

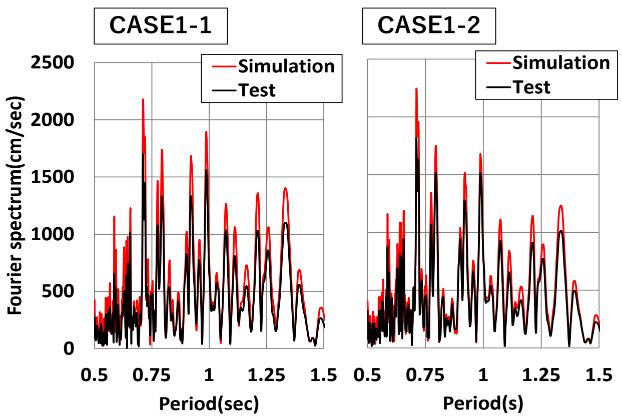

Figure 7. Fourier spectrum of surface ground acceleration.

saturated sand described later, we examined the natural period of dry sand. Figure 5 shows a comparison of the transfer function (the Fourier spectrum ratio) of ground surface acceleration to shaking table acceleration between before and after the main shaking during micro white noise shaking. The natural period of the ground after the main shaking was shortened due to the ground settlement and consolidation in both cases. Furthermore, both before and after main shaking, natural periods of CASE1-2 (high density) were shorter than CASE1-1 (medium density) because ground stiffness becomes greater due to an increase of relative density.

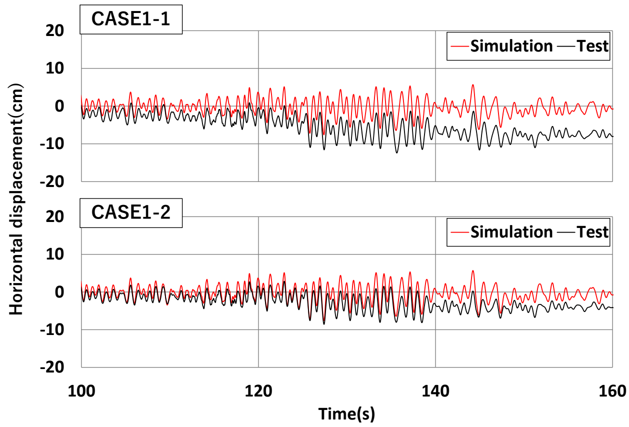

Figure 8. Horizontal displacement of the ground surface (dry sand).

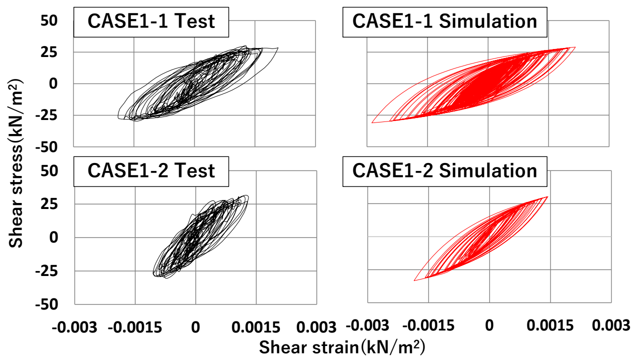

Figure 9. Shear stress-shear strain relationship (dry sand).

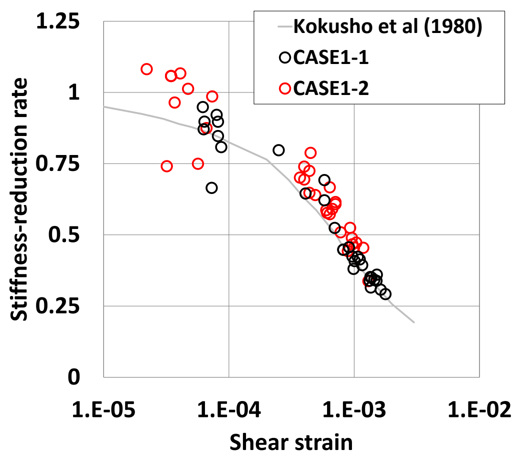

Figure 10. Stiffness-reduction rate.

5.1.2 Surface ground response

Figure 6 shows the time history of ground surface acceleration during the main shaking obtained in the tests and the simulations, focusing on the time around the point of maximum amplitude. Comparing the results of the tests with the results of the simulations, their amplitudes and phases are generally consistent. Figure 7 shows the Fourier spectrum of ground surface acceleration, focusing on 0 to 300 seconds. The period at which the Fourier spectrum reaches its peak is consistent between the tests and the simulations. Between 0.5 and 0.8 seconds, the value in CASE1-2 (high density) is larger than that in CASE1-1 (medium density). On the other hand, between 0.9 and 1.5 seconds, the value in CASE1-1 is larger than that in CASE1-2.

Figure 8 shows the horizontal displacement of ground surface. Horizontal displacements drift in negative direction in both the tests and the simulations. This drift may be due to asymmetry in the input waves, because drift in positive direction occurred in both the tests and the simulations when the model was shaken by a different seismic wave. Comparing CASE1-1 and CASE1-2, the drift magnitude in CASE1-2, where the ground stiffness is greater, is smaller than that in CASE1-1.

5.1.3 Shear stress-shear strain relationships

To further analyze the effect of differences in relative density on the non-linear behavior of the ground, we focused on the shear stress-shear strain relationships. In the tests, shear stress is calculated from the inertial force per unit area of the soil layer shallower than the calculation point, and shear strain is calculated by dividing the relative displacement, which is obtained by double integration of acceleration measured at equal intervals by the separation distance (5m) between accelerometers. When integrating acceleration, a high-pass filter is applied to remove components below 0.2Hz.

Figure 9 shows the shear stress-shear strain relationships between 125 and 150 seconds at G.L.-7.5m. An increase in relative density steepens the slope of the historical loops and reduces their area in both the tests and the simulations. These features clearly reflect differences in non-linear characteristics which are attributable to the difference in relative density of ground.

Figure 10 shows a comparison of the stiffness-reduction rate from the secant stiffness in the tests with the dynamical deformation characteristics of Toyoura sand (Kokusho et al. (1980)). Shear strain is defined as the average of the absolute values of the positive and negative peaks in each loop, expressed as a single-amplitude strain value. The stiffness-reduction rates obtained from the component tests and from these shaking tests show good correspondence.

5.2 Behavior of saturated sand

5.2.1 Natural period of ground

Figure 11 shows a comparison of the transfer function (the Fourier spectrum ratio) of ground surface response acceleration between before and after the main shaking during micro white noise shaking. Similar to CASE1, the natural period after the main shaking was shortened due to ground consolidation, and the natural period in CASE2-2 (high density) was shorter than that in CASE2-1 (medium density).

Furthermore, compared with the natural period in CASE1 with roughly the same relative density, as indicated by the dotted line, the natural period in CASE2 is longer. This is due to a reduction in shear stiffness caused by a decrease in effective confining pressure due to buoyancy and an increase in weight per unit volume caused by the pore fluid.

To verify whether these trends can be reproduced in the simulation model, eigenvalue analyses in which the shear stiffness and the weight per unit volume were set to the values corresponding to saturated sand were conducted. As a result, the natural period is 0.784 seconds in CASE2-1and 0.704 seconds in CASE2-2. These values are close to the natural period before the main shaking in the tests.

5.2.2 Excess pore water pressure

Figure 12 shows a comparison of the time history of excess pore water pressure during and after the main shaking between the tests and the simulations at G.L.-7.5m (shallow part) and G.L.-22.5m (deep part). In CASE2-1 at the deep part, although the dissipation during the main shaking is delayed, the development and dissipation processes in the simulations generally agree with those of the tests.

Focusing on whether excess pore water pressure reaches the initial effective overburden pressure, liquefaction occurred regardless of whether the relative density of ground is medium or high and whether the depth is shallow or deep. Although the figure is omitted, liquefaction occurred at G.L.-27.5m in CASE2-1. This indicates that liquefaction can occur at depths deeper than G.L.-20m, which are excluded from liquefaction assessments in many design guidelines and standards in Japan.

Next, focusing on the dissipation process of excess pore water pressure in the tests, it is evident that the onset time of dissipation is delayed in the shallow part in both cases. This is caused by the supply of pore water from the deep layers to the shallow layers due to the hydraulic gradient created by the difference in excess pore water pressure between the shallow and deep layers. In the simulations, the phenomenon in which the dissipation is completed approximately 10 minutes after the main shaking can be reproduced.

5.2.3 Surface ground response

Figure 13 shows a comparison of the time history of ground surface acceleration between the tests and the simulations. A significant decrease in acceleration

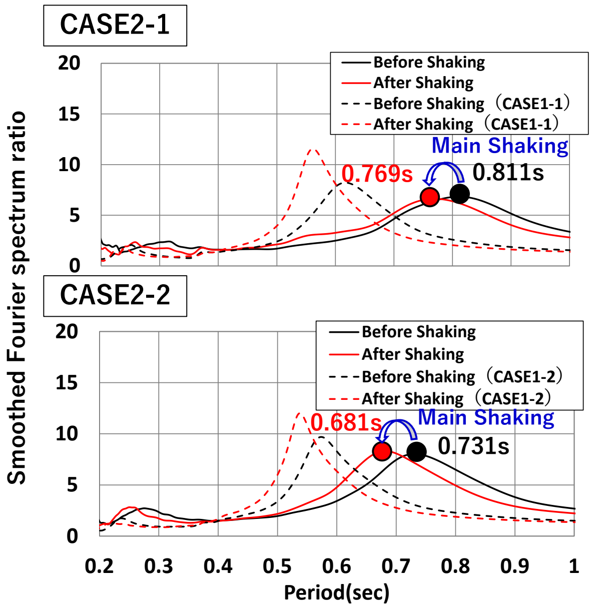

Figure 11. Fourier spectrum ratio (saturated sand).

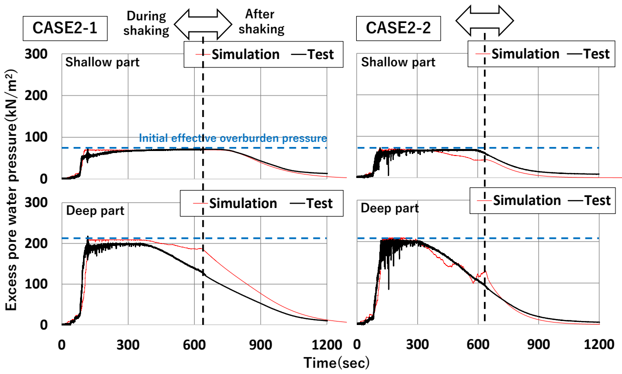

Figure 12. Excess pore water pressure.

amplitude was observed around the time when excess pore water pressure reached the initial effective overburden pressure in both cases, and this trend is generally reproduced in the simulations. Futhermore, large pulsed accelerations were generated due to cyclic mobility in CASE2-2 in the test. The reason why the large pulse was not generated in the simulation is considered to be the influence of damping proportional to stiffness for the sake of stability of the numerical simulation. By adjusting parameters related to damping, we aim in the future to acheive both numerical stability and precise reproduction of acceleration pulses.

Figure 14 shows a comparison of the time history of horizontal displacement of ground surface between the tests and the simulations. The time history of displacement in CASE2-1 (medium density) shows relatively good reproducibility in the simulation. However, in CASE2-2 (high density) the displacement amplitude in the test was extremely large, particularly after 150 seconds, and this trend was not reproduced in the simulation. As mentioned in the last paragraph,

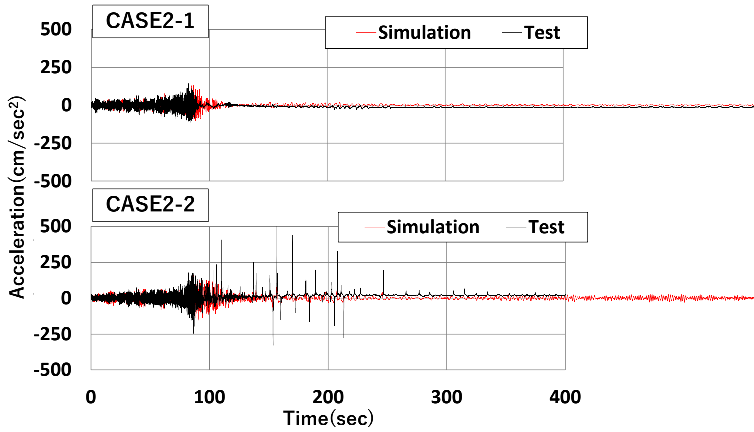

Figure 13. Acceleration of the ground surface (saturated sand).

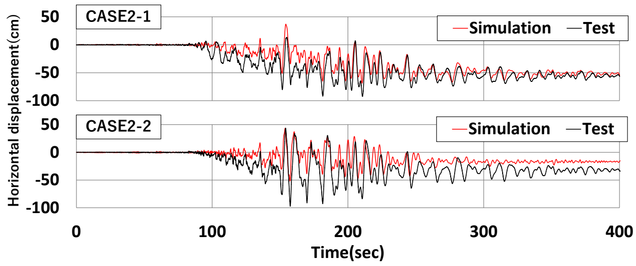

Figure 14. Horizontal displacement of the ground surface (saturated sand).

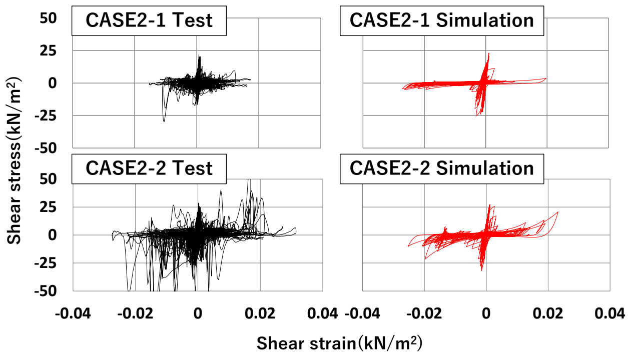

Figure 15. Shear stress-shear strain relationship (saturated sand).

large pulsed accelerations were repeatedly generated due to cyclic mobility after 150 seconds in the test, and they might amplify displacement due to an increase in the inertial force of ground.

5.2.4 Shear stress-shear strain relationship

Figure 15 shows the the shear stress-shear strain relationships between 125 and 150 seconds at the deep part. It indicates that the slope of the historical loop is steep before liquefaction occurs, whereas the slope becomes gentle as strain increases due to stiffness reduction. Furthermore, in CASE2-2, a reverse S-shaped historical loop due to cyclic mobility is clearly observed. These trends can be confirmed in both the tests and the simulations.

As in the case of dry sand, analyzing these relationships clarifies differences in the non-linear characteristics due to the difference in relative density, and enables us to complehend the phenomena occured by cyclic mobility following liquefaction.

6 CONCLUSIONS

The shaking table tests using the new geotechnical centrifuge were conducted to verify the non-linear behavior of sandy soil during a Nankai-Trough simulated earthquake. The findings obtained from the tests are shown in below.

- Focusing on case classification based on whether the ground material is dry or saturated, it is confirmed that the natural period of the ground becomes longer due to the pore fluid and the acceleration of the ground surface is significantly reduced due to the occurrence of liquefaction.
- Focusing on case classification based on the difference in relative density of ground, in the case of dry sand, the natural period of ground was shortened, and the slope of the shear stress-shear strain relationship becomes steeper as relative density increases. In the case of saturated sand, an increase in relative density facilitates cyclic mobility, resulting in the generation of large pulsed accelerations and a reverse S-shaped shear stress-shear strain relationship.
- Moreover, in the test on saturated sand, the possibility of liquefaction occurrence at deep depths, which are excluded from liquefaction assessments in many design guidelines and standards in Japan, during the large and long-period earthquake can be confirmed.

Furthermore, the reproduction simulations targeting the shaking tests were conducted. The results of the simulations generally agree with the results of the tests. In particular, for the simulations targeting saturated sand, incorporating groundwater movement enables reproduction of the development and dissipation processes of excess pore water pressure during long-duration earthquakes such as a Nankai Trough simulated wave.

REFERENCES

The Headquarters for Earthquake Research Promotion (2025). Long-Term Assessment of Earthquake Activity in the Nankai Trough, Ver.2-1 (In Japanese). https://www.jishin.go.jp/main/chousa/kaikou_pdf/nankai_3.pdf

Nagura, K. et al. (1992). A study on the centrifuge model testing. *Taisei Advanced Center of Technology Technical Report*, Vol. 25, pp. 141-148. (In Japanese)

Ghaboussi, J. and Wilson, E, L. (1972): Variational formulation of dynamics of fluid-saturated porous elatic solids, Journal of the Engineering Mechanics Division, ASCE, EM4, pp. 947-963.

Hardin, B.O. and Drnevich, V.P. (1972). Shear Modulus and Damping in Soils. *Design Equations and Curves*, Proc. ASCE, SM7, pp. 667-692.

Cubrinovski, M. and Ishihara, K. (1998). State concept and modified elastoplasticity for sand modelling. *Soils and Foundations*, Vol. 38, No4, pp. 213-225.

Kokusho, T. (1980). Cyclic Triaxial Test of Dynamic Soil Properties for Wide Strain Range. *Soils and Foundations*, Vol. 20, No2, pp. 45-60.

The Architectual Institute of Japan (2019). Recommendations for Design of Building Foundations, ISBN978-4-8189-0652-5, pp. 49-50. (In Japanese)